International Journal of Engineering Research and Development
***e*-ISSN : 2278-067X, *p*-ISSN : 2278-800X, www.ijerd.com**
Volume 12, Issue 12 (December 2016), PP.10-19

Investigation into New Parameter about Dielectric Oil Flow Affecting the Melting Process in EDM

Tomoki Iwata[1], Koichi Hirose[2]
[1]*Technology Development Section, FB Co. Ltd., Japan*
[2]*Research Center for Die and Mold Technology, Iwate University, Japan*

Abstract:- Electrical discharge machining (EDM) is one of the most useful machining methods and widely used especially in a mold manufacturing field. EDM is a thermal process that is caused by discharged plasma generated between a tool electrode and a workpiece. The heat flux from plasma melts a part of workpiece [1], and then a portion of melted workpiece is removed from the workpiece body by several effects [2]-[5] such as super heating [4], [5]. In usual EDM, the tool electrode and the workpiece are submerged in dielectric oil during the machining process. The effects of machining conditions on machining characteristics, such as material removal rate, surface roughness, and tool electrode wear, have been well studied so far. However, the influence of dielectric oil between tool electrode and workpiece on machining process has not been fully understood.

In this study, focusing on the melting process of EDM, a new parameter, named flow conductance, about the oil flow between tool electrode and workpiece was derived from hydrodynamical point of view to investigate the effect of dielectric oil on the process. As a result, the fact that the flow conductance affects the melt volume of workpiece became clear.

Keywords:- EDM, Dielectric oil, Viscosity, Discharge gap, Flow conductance

I. INTRODUCTION

Since electrical discharge machining (EDM) is one of the most useful machining methods to machine the complex cavity form, it is widely used especially in a mold manufacturing field. EDM is a thermal process caused by pulsed discharges generated between the tool electrode and the workpiece that are submerged in dielectric oil. The machining process of EDM consists of two essential processes. One is a melting process of the workpiece, and the other is a removal process of a portion of melted workpiece. In the melting process, the heat flux generated by discharge plasma between electrodes (tool electrode and workpiece) melts a part of the workpiece. The heat flux to the workpiece Q_w is calculated by eq. (1) [6];

$$Q_W(r) = \frac{4.57 \cdot F_W \cdot I \cdot V}{\pi \cdot {R_h}^2} EXP\left(-4.5\frac{r^2}{{R_h}^2}\right) \quad (1)$$

where r is a coordinate in radial direction, F_w is an energy fraction to the workpiece, I is a discharge current, V is a discharge voltage, I·V means a thermal energy generated by the plasma per unit time, and R_h is a heat input radius on the workpiece surface.

Fig.1 shows a single pulse discharge phenomena observed by high speed video camera, which is ignited between needle shaped copper electrode and carbon steel workpiece. Electrodes were submerged in the dielectric oil like usual EDM. In Fig. 1, the evaporation of dielectric oil generates an expanding bubble right after the dielectric breakdown. Fig. 1 also shows that the plasma column is covered with the bubble. In actual EDM process, the repetitions of discharge as shown in Fig.1 machine the workpiece into inverted form of the tool electrode shape.

Authors [7] investigated about the melt depth of workpiece and the removal efficiency, a ratio of removed depth to melt depth, using nine types of commercial dielectric oil. Fig. 2 shows variation in melt volume (=melt depth × machined area) between oils and Fig. 3 shows variation in removal efficiency between oils. The melt volume varies from $7.6\times10^4 \mu m^3$ to $11.2\times10^4 \mu m^3$ depending on oil type in Fig. 2, while the removal efficiencies are almost the same in Fig. 3.

Since the melt volume of workpiece is unquestionably affected by the heat flux shown in eq. (1), the heat input radius has an effect on the melt volume of workpiece. Several literatures [1], [8], [9] reported about the heat input radius or the plasma diameter that is directly related to the heat flux. One of authors [1] reported that the different type of dielectric oil causes the different heat input radius at the workpiece surface. Kunieda [8] studied that the plasma diameter in air completes its expansion within 2μs after dielectric breakdown. On the other hand, Kojima et al. [9] observed the plasma expansion in oil by means of high speed video camera and reported that the plasma expansion speed in oil is much slower than the expansion speed in air. These literatures [1], [8], [9] mean that the dielectric fluid around the plasma column, such as oil or air, probably suppresses the

plasma column expansion due to its hydrodynamical damping effect. In the case of dielectric oil is used, the oil suppresses the bubble expansion, suppressing the plasma column expansion.

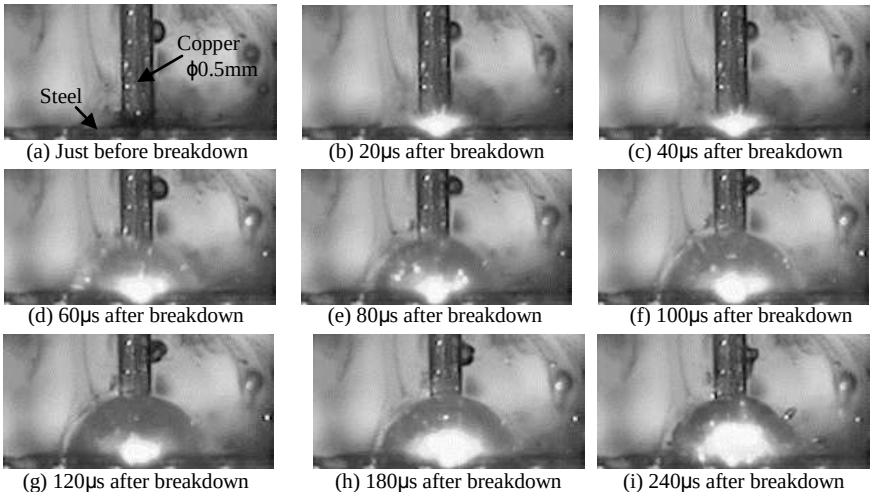

Fig. 1: Single pulse discharge phenomenon with the passage of discharging time observed by high speed video camera

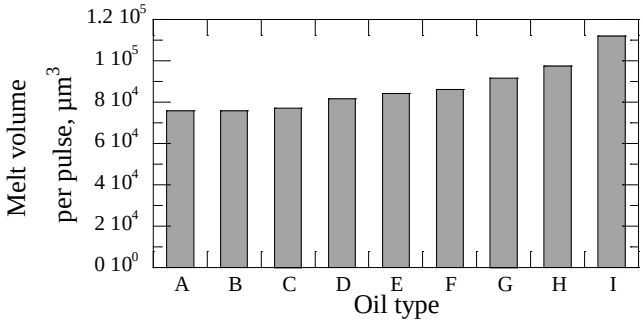

Fig. 2: Variation in melt volume per pulse – workpiece (cathode) material: steel, tool electrode material: copper, discharge current: 10A, discharge duration: 250μs, pulse interval time: 250μs, machining time: 4min.

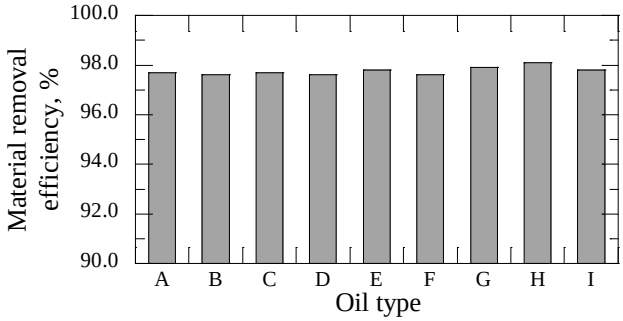

Fig. 3: Variation in material removal efficiency – workpiece (cathode) material: steel, tool electrode material: copper, discharge current: 10A, discharge duration: 250μs, pulse interval time: 250μs, machining time: 4min.

In this study, a new parameter that means flowing ability of oil between electrodes was derived first from the hydrodynamical point of view. In the next place, experiments were carried out to calculate actual value of the derived parameter, using three types of dielectric oil (oil A, G, and I). Finally, the relationship between new parameter and the melt volume of workpiece was discussed.

II. DERIVATION OF NEW PARAMETER

A. Oil Flow around the Bubble

As described in chapter I, the bubble is generated around the discharge point right after the dielectric breakdown, beginning to expand radially. This means the oil around the bubble flows radially also. In this section, the considering result of how oil flows is described.

Hayakawa et al. [10] carried out the single discharge experiment to observe the bubble expanding behavior with discharge current of 30A and discharge duration of 200μs. In the experiment, the parallel flat gap space was composed of a metal rod electrode and a transparent plate in which a metal wire electrode was inserted. Hayakawa et al. [10] observed expanding bubble behavior through the transparent plate using high speed video camera to measure the time variation of expanding bubble diameter.

The bubble expanding model, to calculate the oil flow velocity around the bubble using the data of Hayakawa et al. [10], is shown in Fig. 4. In the bubble expanding model, two assumptions are employed. One assumption is that the bubble is column-shaped, and the other is that the bubble expands concentrically, moving the oil only to the radial direction.

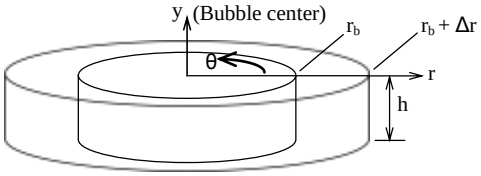

Fig. 4: Bubble expanding model

In Fig. 4, the oil flow around the bubble, caused by the bubble expansion from r_b to $r_b + \Delta r$, is expressed as follows;

$$\begin{aligned} F &= h\pi(r_b + \Delta r)^2 - h\pi r_b{}^2 = h\pi\left(2r_b\Delta r + \Delta r^2\right) \\ &= 2h\pi r_b \Delta r \\ &= 2h\pi r_b v_b dt \\ &\because 2r_b\Delta r >> \Delta r^2 \\ &\because \Delta r = v_b dt \end{aligned} \tag{2}$$

where F is a flow volume of oil, r_b is a bubble radius, Δr is an increment of a bubble radius, h is a distance between electrodes, v_b is a bubble expanding velocity in the radial direction. Since the oil flows only to the radial direction, the flow velocity of oil at $r=r_x$ ($>r_b$) is expressed as follows;

$$2h\pi r_b v_b dt = 2h\pi r_x v_x dt \tag{3}$$

$$v_x = \frac{r_b}{r_x} v_b \tag{4}$$

where v_x is oil flow velocity at $r=r_x$ ($>r_b$).

The flow velocity of oil, near the bubble-oil interface, calculated using eq. (4) is shown in Fig. 5. In this figure, the oil flow can be considered as a steady flow until 200μs after ignition because the time variation in flow velocity are small. At 250μs after ignition, the flow velocity decreases rapidly. Therefore, the oil flow between electrodes is considered as a steady flow from at least 50μs after ignition until the discharge is terminated.

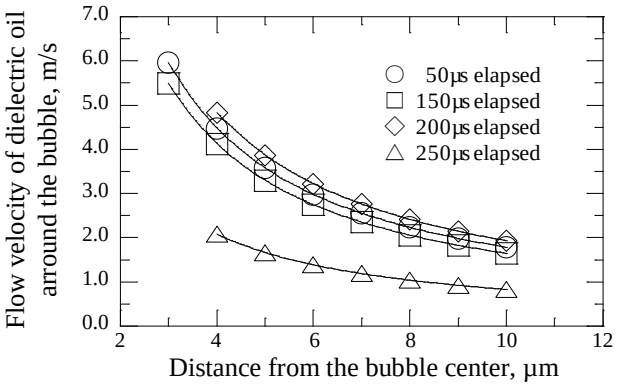

Fig. 5: Flow velocity of dielectric oil arround the bubble – workpiece (cathode) material: steel rod, tool electrode material: copper wire, discharge current: 30A, discharge duration: 200μs, discharge gap: 10-30μm

Moreover, literature [10] shows that the bubble diameter expands to several millimeters concentrically in 100μs, which is two-digits larger than the distance between electrodes, therefore, the oil flow in z-direction

and θ-direction can be ignored. As a result of consideration, the oil flow between parallel plane electrodes is considered as a steady and laminar flow to the radial direction.

B. Flow Conductance

Ignoring external forces such as gravity, the forces that act on a volume of flowing oil are a pressure and a viscous frictional force. As described in section II.-A., the oil flow between parallel plane electrodes is considered as a steady and laminar flow to the radial direction. In the steady and laminar flow, the forces in the radial direction (pressure force and viscous frictional force) are balanced.

Fig. 6 shows the oil flow model between parallel plane electrodes. In this model, the balance of the forces in the radial direction is expressed as follows;

$$p(rd\theta dy)-\left(p+\frac{dp}{dr}dr\right)(r+dr)d\theta dy+2p\cdot\sin\left(\frac{d\theta}{2}\right)drdy-\tau(rd\theta dr)+\left(\tau+\frac{d\tau}{dy}dy\right)(rd\theta dr)=0 \quad (5)$$

where y is coordinate in discharge gap direction, r is coordinate in radial direction, θ is coordinate in circumferencial direction, p is pressure, τ is shear stress.

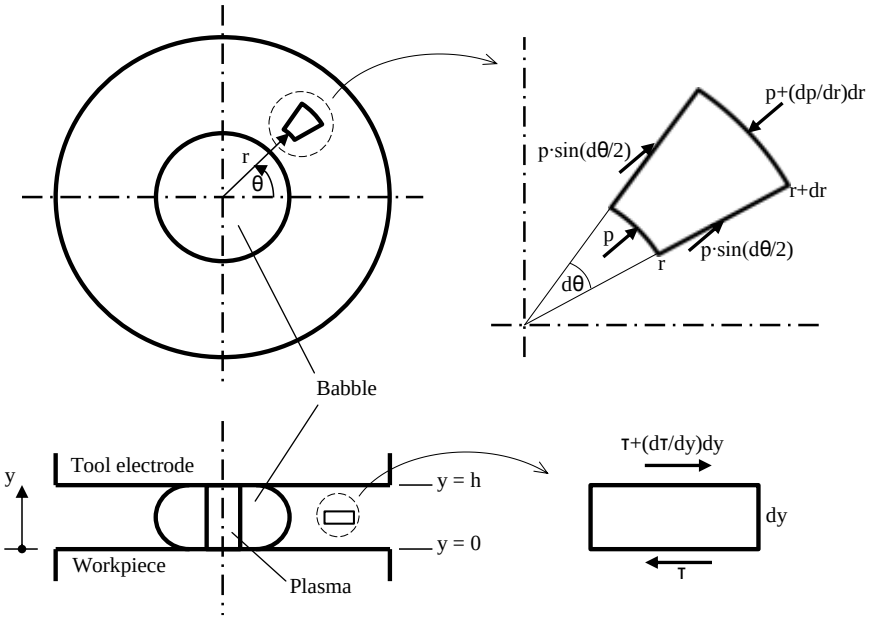

Fig. 6: Radial force equilibrium model of dielectric oil between electrodes

As Hinduja et al. [11] noted, the oil flow between parallel plane electrodes is considered as Poiseuille flow that has a parabolic distribution of flow velocity along vertical direction. In Poiseuille flow as shown in Fig. 6, the boundary conditions of flow velocity in radial direction at y=0 and y=h can reasonably be taken as zero. Applying approximation of $\sin(d\theta/2) \approx d\theta/2$, Newton's law of viscosity ($\tau=\mu\cdot du/dy$), and the boundary conditions in Poiseuille flow to eq. (5), the radial flow velocity u is calculated as follows.

$$u=\frac{1}{2\mu}\left(-\frac{dp}{dr}\right)(h-y)y \quad (6)$$

Since micro flow volume (dF) of oil at r is calculated by;

$$dF=2\pi rudy \quad (7)$$

the flow volume F is calculated as follows;

$$F=\int_0^h(2\pi r)udy=\frac{\pi h^3}{6\mu}\left(-\frac{dp}{dr}\right)r=C_f\left(-\frac{dp}{dr}\right)r \quad (8)$$

where F is flow volume, and μ is viscosity. In eq. (8), C_f is calculated as follows.

$$C_f=\frac{\pi\cdot h^3}{6\mu} \quad (9)$$

In eq. (8), C_f means the ease of flowing of oil between electrodes, which is calculated by discharge gap h and oil viscosity μ. In this study, C_f is designated as 'flow conductance'. The oil between electrodes becomes difficult

to flow with decrease of flow conductance, suppressing the bubble expansion. This phenomenon causes the heat flux on the workpiece surface to increase, which further enhances the workpiece melting capability.

C. Pressure Gradient

Since eq. (8) includes the pressure gradient (dp/dr) term, the changes in the internal pressure of bubble, generated right after the dielectric breakdown, were also investigated in this study. Three oils of A, G, and I that are shown in Fig. 1 and Fig. 2 were used for the investigation.

The oil around the plasma is evaporated in the instant of dielectric breakdown. Since the oil changes its phase from liquid to gas rapidly without enough time to expand its volume, high pressure of the gas is generated instantaneously. To estimate the value of this high pressure, the analyses of the components for respective oils by GC-MS (gas chromatograph mass spectrometer) were carried out.

Fig. 7 show TIC (Total Ion Chromatogram) graphs measured by GC-MS equipment. The mass spectrum library search, which is a function of GC-MS equipment, revealed that the main components of oil A, G, and I are hydrocarbons of methane series ($CH_3(CH_2)_{n-2}CH_3$, n=11~19).

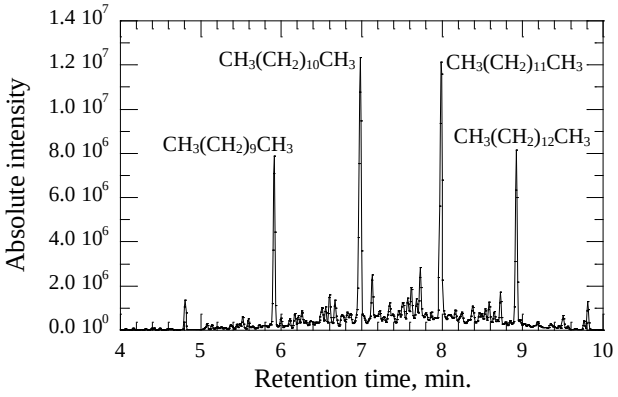

(a) Total ion chromatogram of oil A

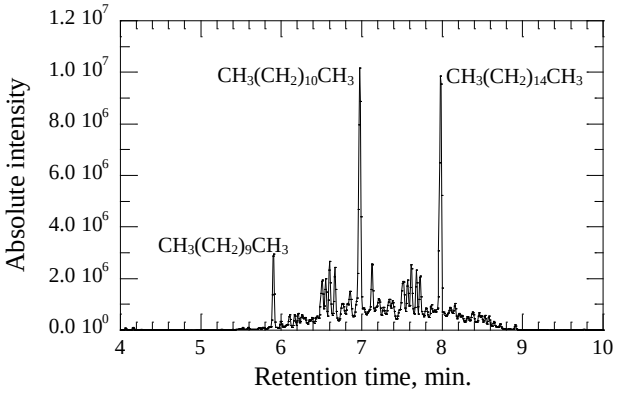

(b) Total ion chromatogram of oil G

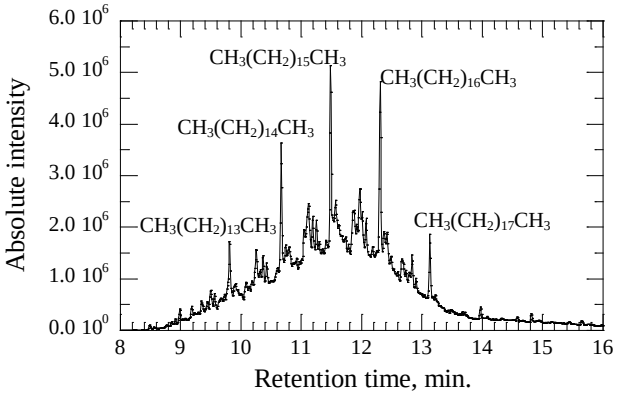

(c) Total ion chromatogram of oil I

Fig. 7: Total ion chromatogram measured by gas chromatograph mass spectrometer

The gas pressures at the instant of oil evaporation for respective main components of oils were calculated on the assumption that the gasses are ideal. The results are shown in Fig. 8. This result shows that respective pressures are in the range of 14.5 to 18.2 MPa (16.35 MPa ±11.3%). These variations in pressure are insignificant to flow volume F in eq. (8) by comparison with variations in flow conductance described in the next chapter. The physicochemical properties used for the pressure calculation are shown in Table I.

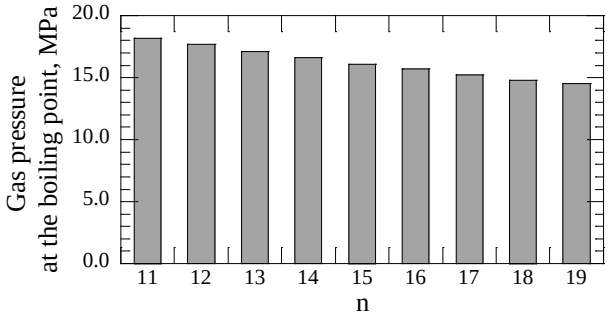

Fig. 8: Gas pressure at boiling point of hydrocarbon of methane series $CH_3(CH_2)_{n-2}CH_3$

Table I: Physicochemical properties of methane series $CH_3(CH_2)_{n-2}CH_3$

n	Boiling point, K	Density at 293K, g/cm^3	Molecular weight
11	469	0.740	156.31
12	489	0.749	170.33
13	508	0.756	184.36
14	527	0.763	198.39
15	544	0.769	212.41
16	560	0.773	226.44
17	575	0.778	240.47
18	589	0.777	254.49
19	603	0.786	268.52

III. CALCULATION OF FLOW CONDUCTANCE

A. Oil Viscosity Measuring

To calculate the flow conductance in eq. (8), oil viscosity and discharge gap were measured. The measuring results about the oil viscosity is described in this section and the measuring result about the discharge gap is described in next section. Fig. 9 shows the temperature characteristics of oil viscosity measured by tuning fork vibro viscometer. The oil viscosity decreases with increase of oil temperature.

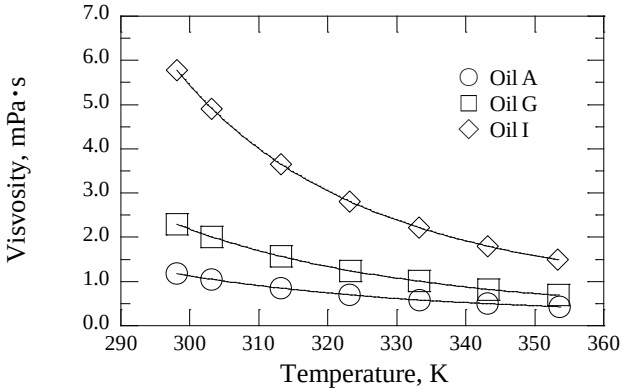

Fig. 9: Temperature characteristic of oil viscosity

In the actual EDM process, the temperature at the bubble-liquid interface is approximately boiling point of the oil. The temperature distribution around the bubble-liquid interface was calculated by means of transient one-dimensional thermal conduction analysis. The results of the analysis are shown in Fig. 10. This calculated result shows that the oil temperature decreases rapidly with increase of distance from the bubble-oil interface (x=0). When 250μs elapsed after the dielectric breakdown, the oil temperature at the point where only 15μm away from the bubble-liquid interface remains unchanged.

Since the temperature of most volume of the oil between electrodes keeps the initial temperature during discharge duration (250μs), oil viscosity at initial temperature (296K) was employed for the calculation of flow conductance in this study.

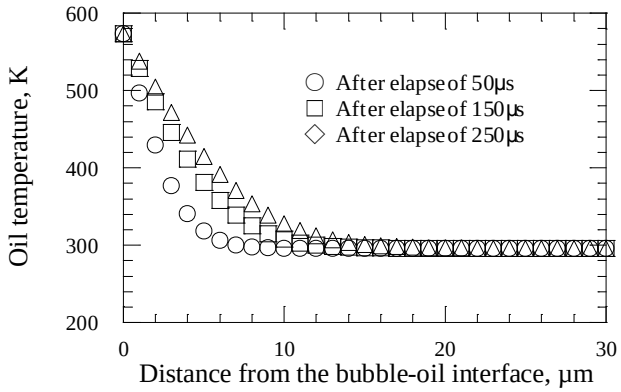

Fig. 10: One-dimensional analytical results of oil temperature around the bubble-liquid interface – Analysis range: 0 to 5000μm, Δx: 1μm, Δt: 1μs, thermal diffusivity: $8.0\times10^{-8}m^2/s$, initial condition: 296K, boundary condition at x=0: 573K, boundary condition at x=5000μm: 296K

B. Discharge Gap Measuring

The servo reference voltage that is one of the machining conditions in EDM controls the discharge gap. Higher servo reference voltage causes wider discharge gap and lower servo reference voltage makes the discharge gap narrower in general. Two terms such as 'distance' and 'gap' are used in this section. The term of 'distance' means raw data of a distance between electrodes measured by the method described in this section. The distance was measured five times for the same servo reference voltage. The term of 'gap' means average value of five distance data. The discharge distance was measured with the laser displacement sensor to investigate the relationship between the servo reference voltage and the discharge gap. The setup for discharge distance measuring is shown in Fig. 11.

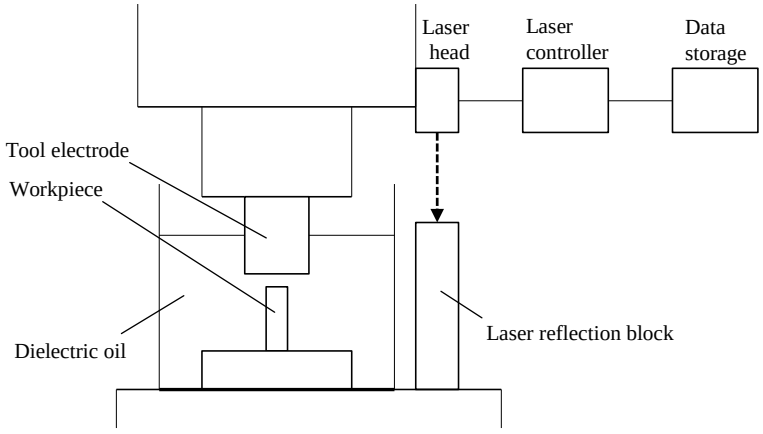

Fig. 11: Measuring setup for inter-electrode distance

Before the discharge distance measuring, the tool electrode was moved toward the workpiece slowly while measuring electrical resistance between electrodes. The distance between electrodes was set to be zero when the electrical resistance had reached a minimum value. Then, the machining for displacement measuring was started with the machining conditions shown in Table II. During the machining, the displacement of the tool electrode was measured with the laser displacement sensor. The example of measured data is shown in Fig. 12. The mean value of displacement data from 0.9s through 1.3s was defined as discharge distance. The discharge

distance was measured five times for respective servo reference voltages shown in Table II, then the average value of five discharge distances was figured out as discharge gap. The relationship between servo reference voltage and discharge gap is shown in Fig. 13.

Table II: Machining conditions for electrodes distance measuring

Item	Description
Tool electrode material	Copper
Workpiece material	Steel
Open circuit voltage	90 V
Discharge current	10 A
Discharge duration	250 μs
Pulse interval	250 μs
Workpiece polarity	Cathode
Servo reference voltage	15, 20, 40, 60 V
Dielectric oil	Oil A, G, I

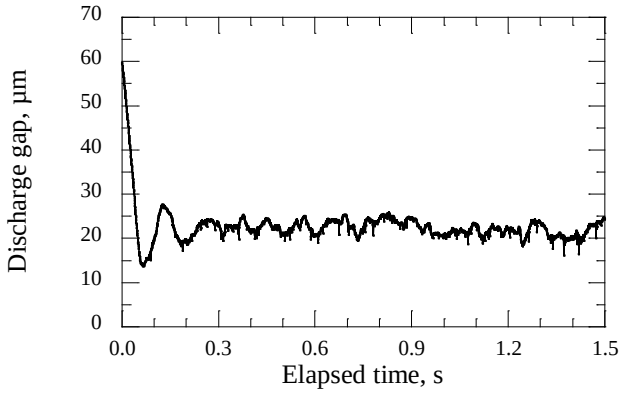

Fig. 12: Measuring example of distance between electrodes with passage of machining time

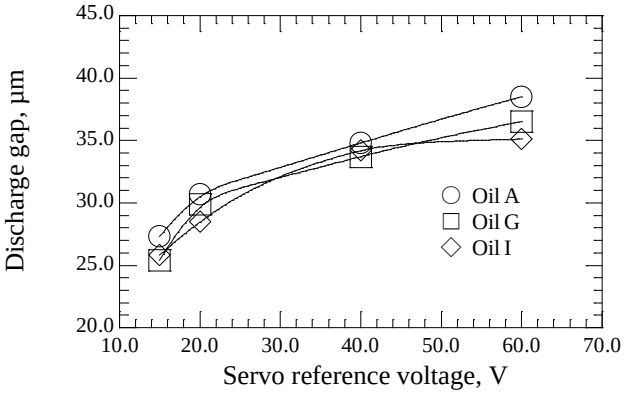

Fig. 13: Relationship between servo reference voltage and discharge gap

C. Calculation of Flow Conductance

Fig. 14 shows the flow conductance that is calculated by substituting the oil viscosity at 296 K (Fig. 9) and the discharge gap (Fig. 13) into eq. (9). The flow conductance increases with increase of discharge gap, and it decreases with increase of oil viscosity. In the following chapter, the relation between the flow conductance calculated here and the melt volume per pulse shown in Fig. 2 is given, and the mechanism of how the flow conductance affects the melt volume per pulse is discussed.

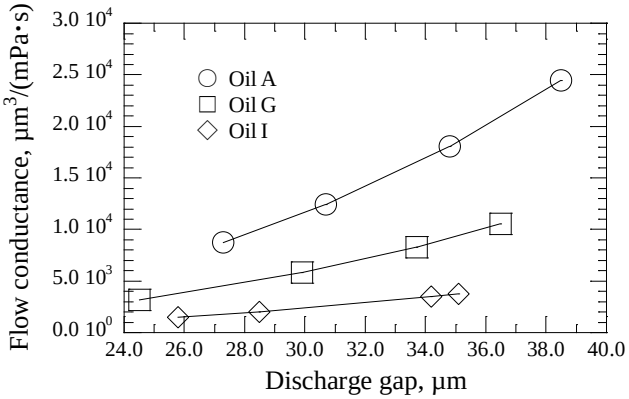

Fig. 14: Relationship between discharge gap, oil viscosity, and flow conductance

IV. DISCUSSIONS

The relationship between flow conductance and melt volume is shown in Fig. 15. It shows that the melt volume increases with decreasing of the flow conductance. Fig. 16 is the explanation of the effect of flow conductance. When the flow conductance decreases, the bubble expansion is suppressed, making the heat input radius smaller. As a result, the heat flux to the workpiece increases, which in turn increasing the melt volume of the workpiece.

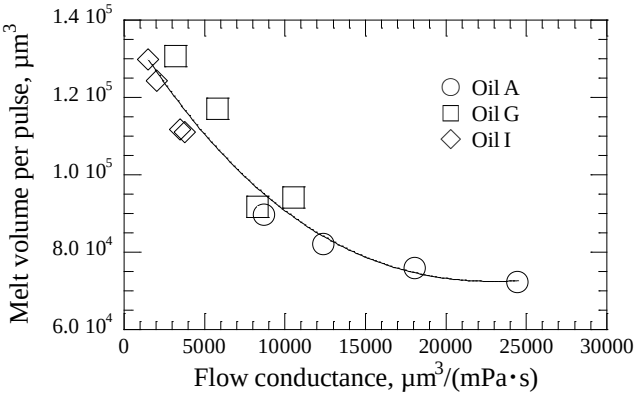

Fig. 15: Relationship between flow conductance and melt volume per pulse (see Fig. 2)

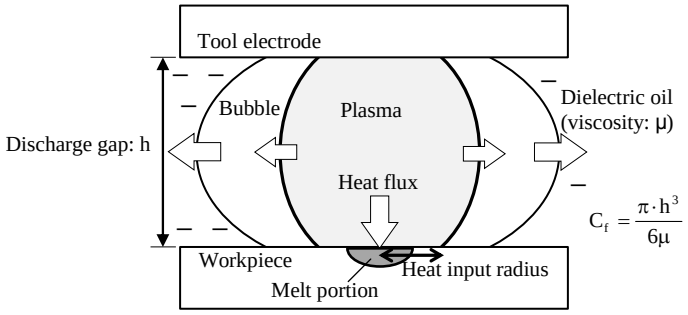

Fig. 16: Explanation of the effect of flow conductance C_f – In the case of C_f is smaller, the bubble expansion is suppressed, which makes the plasma diameter smaller. As a result of this phenomenon, the heat input radius decreases, causing the heat flux to workpiece increases, which in turn increases the melt volume of workpiece.

V. CONCLUSIONS

EDM consists of two main processes such as melting process and removal process. In this study, focusing on the melting process, the new parameter that probably affects the melting volume of the workpiece was derived from the hydrodynamical point of view. This new parameter is designated as 'flow conductance' that is calculated by oil viscosity and discharge gap. The effect of flow conductance on the melt volume of

workpiece was experimentally proved in this study. As a result of this study, it has become clear that the smaller flow conductance causes larger melt volume of the workpiece.

The flow conductance introduced in this study is an original idea. As far as authors know, there is no paper that investigates the effect of oil flow on the melt volume of workpiece quantitatively. Authors are confident that the effect of flow conductance contributes to progress EDM capability in the future.

ACKNOWLEDGMENT

The authors are very grateful to Dr. Akira Iwabuchi, the president of Iwate University, for the support rendered. Without his guidance and persistent help, this paper would not have been possible.

REFERENCES

[1]. Tomoki Iwata, "New Thermo-Physical Modeling of EDM with Latent Heat Consumption," International Journal of Engineering Research and Development, Vol. 12, No. 7 (2016) pp. 54-63

[2]. A. Singh and A. Ghosh, "A thermo-electric model of material removal during electric discharge machining," International Journal of Machine Tools and Manufacture, Vol. 39, No. 4 (1999) pp. 669-682

[3]. T. O. Hockenberry and E. M. Williams, "Dynamic Evolution of Events Accompanying the Low-Voltage Discharge Employed in EDM," IEEE Transactions on Industry and General Applications, Vol. IGA-3, No. 4 (1967) pp. 302-309

[4]. B. N. Zolotykh, "The Mechanism of Electrical Erosion of Metals in Liquid Dielectric Media," Soviet Physics-Technical Physics, Vol. 4, No. 12 (1959) pp. 1370-1373

[5]. P. T. Eubank, M. R. Patel, M. A. Barrufet, and B. Bozkurt, "Theoretical models of the electrical discharge machining process. III. The variable mass, cylindrical plasma model," Journal of Applied Physics, Vol. 73, No. 11 (1993) pp. 7900-7909

[6]. S. N. Joshi and S.S. Pande, "Thermo-Physical modeling of die-sinking EDM process," Journal of Manufacturing Processes, 12 (2010) pp. 45-56

[7]. Tomoki Iwata and Koichi Hirose, "Experimental Study of Material Removal Efficiency in EDM Using Various Types of Dielectric Oil," International Journal of Engineering Research and Development, Vol. 11, No. 8 (2015) pp. 34-41

[8]. M. Kunieda, "Advancements in Fundamental Studies on EDM Gap Phenomena," Proceedings of the 16th International Symposium on Electromachining, (2010) pp. 15-23

[9]. A. Kojima, W. Natsu, and M. Kunieda, "Spectroscopic measurement of arc plasma diameter in EDM," CIRP Annals – Manufacturing Technology, 57 (2008) pp. 203-207

[10]. Shinya Hayakawa, Teruya Doke, Fumihiro Itoigawa, and Takashi Nakamura, "Observation of Bubble Expansion and Flying Debris in Parallel Flat Gap Space in Electrical Discharge Machining," International Journal of Electrical Machining, 14 (2009) pp. 29-35

[11]. S. Hinduja and M. Kunieda, "Modelling of ECM and EDM processes," CIRP Annals – Manufacturing Technology, 62 (2003) pp. 775-797